JOURNAL OF MATERIALS SCIENCE 37 (2002) 723–730

Crystallisation of M-SiAlON glasses to I_w-phase glass-ceramics: preparation and characterisation

A. DIAZ, S. HAMPSHIRE
Ceramics Research Unit, Materials and Surface Science Institute, University of Limerick, Limerick, Ireland
E-mail: aranzazu.diaz@ul.ie

The crystallisation of M-SiAlON glasses (M = Y, Ln) is particularly sensitive to small variations in composition and heat treatment temperature. The formation of I_w-phase in the YSiAlON system has been studied but little information concerning its nucleation, thermal stability, mechanical properties and extension into the lanthanide sialon series is available. In order to better understand the synthesis and to characterise more fully the I_w-glass-ceramic materials, a series of glass compositions have been prepared and characterised. These include $M_3Si_3Al_2O_{12.15}N_{0.90}$ (M = Y, Er, Ce, Yb); $M_{3.45}Si_3Al_2O_{12.76}N_{0.95}$ (M = Y, Er); $Y_4Si_3Al_2O_{13.50}N$ and $Y_4Si_{3.37}Al_{1.50}O_{13.50}N$. Heat treatments were performed on these glasses and the resulting crystalline products have been studied by X-ray diffraction (XRD). Differential Thermal Analysis (DTA) in combination with XRD analysis of $Y_{3.45}Si_3Al_2O_{12.76}N_{0.95}$ and $Ce_3Si_2Al_2O_{12.15}N_{0.90}$ parent glass-compositions was used to investigate crystal phase formation. Young's modulus (E), hardness (H_v) and fracture toughness (K_{IC}) of the glass-ceramics were measured. Glass-ceramics containing I_w-phase as the only detectable crystalline phase have been produced from $M_3Si_3Al_2O_{12.15}N_{0.90}$ and $M_{3.45}Si_3Al_2O_{12.76}N_{0.95}$ (M = Y and Er) compositions. No equivalent phase was found in the Ce- and Yb-sialon compositions.

1. Introduction

The crystallisation of yttrium and lanthanide oxynitride glasses has been investigated principally in view of their role as grain boundary phases in silicon nitride based ceramics. Numerous five component phases have been reported in various M-SiAlON systems (M = Y, La, Ce, Nd, Sm, Gd, Dy, Er, Yb) [1–4]. However, some of them have been poorly characterised due to the problems of preparing them in a pure form. One of the most commonly observed low temperature devitrification products is known as B-phase (Y_2SiAlO_5N). Although this phase lies outside the glass forming region, it has been found that appropriate combinations of starting compositions and crystallisation heat treatments result in the formation of B-phase as a single crystalline phase [5–7].

B-phase is only stable up to about 1100°C and, above this temperature, a second apparently structurally related phase, designated I_w, occurs [8]. This phase, was first observed in the YSiAlON system using Scanning Electron Microscopy (SEM) techniques by Leng-Ward and Lewis [9, 10] who found a cation ratio of Y : Si : Al = 3 : 2 : 1 by EDX analysis in the SEM [9], and 5 : 3 : 2 by EDX analysis in the TEM [10]. Analysis of the X-ray diffraction pattern of I_w shows strong peaks close to B-phase but with numerous additional superlattice reflexions which suggested to Liddel *et al.* [8] that I_w had a wollastonite structure for which the (Si + Al) : (O + N) ratio was 1 : 3. Using the $Y_3Si_3Al_2O_{12.15}N_{0.90}$ (10 e/o N) starting composition, these authors identified, after devitrification at 1150°C, I_w as a single crystalline phase with some residual glass remaining [4].

Subsequent studies [11] were carried out using materials with a starting composition of $Y_xSi_3Al_2O_{13.5y}N_y$ with $x = 3.45$, 3.90 and 4.33 and a nitrogen content of 10 e/o. The samples were melted and quenched directly to the temperature range of 1150–1250°C. For $x = 3.45$, B-phase was always present, and for high Y content ($x > 3.45$), J-phase (Y_4SiAlO_8N) formed preferentially. I_w-phase formation has been associated with the formation of B-phase [11], suggesting that I_w occurs by transformation of previously nucleated B-phase.

In the present work, in order to continue the study of I_w phase in the yttrium sialon system, four glasses (10 e/o N), $Y_3Si_3Al_2O_{12.15}N_{0.90}$, $Y_{3.45}Si_3Al_2O_{12.76}N_{0.95}$, $Y_4Si_3Al_2O_{13.50}N$, and $Y_4Si_{3.37}Al_{1.50}O_{13.50}N$ have been prepared. These parent glasses have been characterised and crystallisation studies have been carried out.

Analysis of the crystalline products resulting from heat treatment studies in the yttrium and other lanthanide sialon systems revealed that phase relationships and stability are dependent not only upon temperature and composition but also upon cation size. Glass compositions, 10 e/o N, using erbium ($Er_3Si_3Al_2O_{12.15}N_{0.90}$, $Er_{3.45}Si_3Al_2O_{12.76}N_{0.95}$), cerium and ytterbium ($M_3Si_3Al_2O_{12.15}N_{0.90}$) have been prepared and characterised. In order to determine

whether I_w-phase extends into the lanthanide series, crystallisation studies have also been performed with characterisation of the resulting materials.

2. Experimental procedure

2.1. Compositions and materials preparation

2.1.1. Glass preparation

Glass compositions with varying cation ratios M : Si : Al = 3 : 3 : 2 (M = Y, Ce, Er, Yb); M : Si : Al = 3.45 : 3 : 2 (M = Y, Er); M : Si : Al = 4 : 3 : 2 and 4 : 3.37 : 1.5 (M = Y); containing 10 e/o N (e/o N = 3[N]10^2/(3[N] + 2[O]) [12] were prepared from mixtures of high purity powders of Si_3N_4 (HC Starck), SiO_2 (Fluka Chemika), Al_2O_3 (Aldrich Chemicals) and Y_2O_3 (HC Starck) or CeO_2 (Alfa), Er_2O_3 (Alfa) and Yb_2O_3 (Reacton). Glass compositions are showed in Fig. 1. The powders were ball milled using isopropanol for 24 h and pressed into compacts by cold isostatic pressing. The compacts were then melted for 1 h at 1715°C in a boron nitride lined graphite tube furnace under flowing nitrogen at 0.1 MPa. The melt was then quickly removed and poured into a pre-heated graphite mould followed by annealing at 850°C for 1 hour and then slow cooled in the furnace to room temperature.

2.1.2. Heat treatments

Crystallisation studies using a one-stage heat treatment of ten hours at 1050, 1100, 1150 and 1200°C were conducted on these glasses under a nitrogen atmosphere. Glass samples of $15 \times 5 \times 3$ mm^3 were placed in a bed of boron nitride within an alumina crucible. The crucible was then placed in a horizontal tube furnace which was then evacuated, before introducing nitrogen at 0.1 MPa. YSiAlON glasses are self nucleating and it has been shown [13] that without any addition of nucleating agents, it is possible to obtain appreciable crystallisation with a very fine microstructure. Samples were heated at 20°C min^{-1} directly to the crystallisation temperature (between 1050 and 1200°C), held for 10 hours and then cooled in the furnace at 10°C min^{-1}.

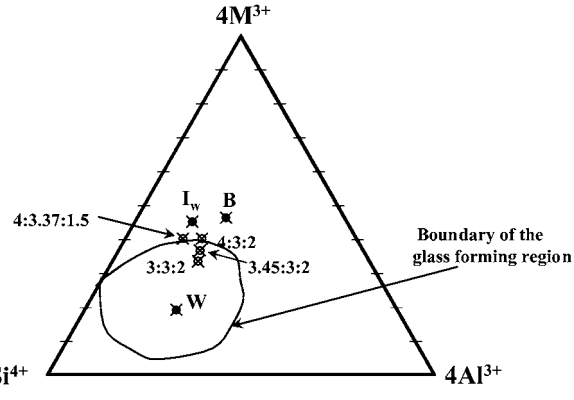

Figure 1 Section of Jäneque prism corresponding to 10 e/oN with the approximate glass-forming region marked [12, 24], showing the parent glass compositions used with M : Si : Al = 3 : 3 : 2; 3.45 : 3 : 2; 4 : 3 : 2; 4 : 3.37 : 1.5 and B, I_w (M : Si : Al = 3 : 2 : 1) and W phase stoichiometries.

Precautions were taken to avoid any possible oxidation layer before undertaking X-ray diffraction analysis and measurements of density, elastic modulus, hardness and fracture toughness.

2.2. Characterisation

2.2.1. Bulk physical and mechanical properties

The bulk density was measured by an Archimedean displacement technique using distilled water. The elastic moduli for the glass ceramics were determined at room temperature from measurements of the longitudinal, V_l, and transverse, V_t, ultrasonic velocities using the method of McSkimmin and Fisher [14]. These velocities were determined using two specially designed 10 MHz piezoelectric transducers. The Young's modulus, E was derived from Equation 1 [14].

$$E = \rho\left[3V_l^2 - 4V_t^2\right]/\left[\left(V_l^2/V_t^2\right) - 1\right] \quad (1)$$

Microhardness testing was carried out on appropriate polished samples using a LECO (M400 G1) Microhardness Tester with a 136° Diamond Pyramid Indenter (Vickers Indenter) and calculated by measuring the impression half-diagonal and using Equation 2 [15],

$$H_v = 463.6P/a^2 \text{ (GPa)} \quad (2)$$

where P = load applied (N), a = length of impression of half-diagonal (μm).

Fracture toughness, K_{IC} was evaluated from the Vickers indentation by the method described by Anstis *et al*. [16]. Care was taken to ensure the load was sufficient to induce penny-cracks and unacceptable crack patterns were excluded. K_{IC} values were calculated using Equation 3,

$$K_{IC} = 0.016E^{0.5}H^{-0.5}Pc^{-1.5}(\times 10^{-6})(\text{MPa m}^{1/2}) \quad (3)$$

where H = hardness (GPa), E = Young's Modulus (GPa) and c = average crack length (m).

2.2.2. Thermal analysis

Differential thermal analysis (DTA) was carried out in a Stanton-Redcroft STA1640 simultaneous TG/DTA analyser. Samples of 60 mg were heated at 5 and 20°C min^{-1} up to the appropiate temperature in boron nitride-lined platinum crucibles in a flowing nitrogen atmosphere. Al_2O_3 was used as the reference material. The midpoint of the endothermic drift on the DTA curve is reported as T_g.

Thermal expansion coefficient was measured in a Netzsch (402EP) dilatometer in air on glass bars prepared with a length of 10 mm. The temperature was increased at a rate of 5°C min^{-1}. The thermal expansion coefficient (α) was calculated between 200 and 800°C using Equation 4,

$$\alpha = (\Delta l/l_0)/\Delta T \quad (4)$$

TABLE I Mechanical and thermal properties of M-SiAlON glasses (standard deviations are shown in brackets)

M	CFS ($Å^{-2}$)	Composition (M : Si : Al)	X-Ray analysis	Colour	ρ (g cm^{-3})	E (GPa)	H_v (GPa)	K_{IC} ($MPam^{1/2}$)	$T_{g_{Dil}}$ (°C)	$\alpha_{(200-800)}$ $\times 10^6$ (K^{-1})	$T_{g_{DTA}}$ (°C)	T_{c1} (°C)	T_{c2} (°C)
Y	2.77	3 : 3 : 2	Amorphous	Grey	3.89	143	8.8 (0.3)	1.4 (0.2)	909	7.18	923	1067	1137
		3.45 : 3 : 2	Amorphous	Grey	3.95	143	8.9 (0.3)	1.4 (0.1)	897	7.55	921	1048	1132
		4 : 3 : 2	Amorphous	Grey	4.12	150	–	–	906	7.85	935	1053	1145
		4 : 3.37 : 1.5	Amorphous	Grey	4.14	151	–	–	910	8.03	942	1069	1153
Ce	2.27	3 : 3 : 2	Amorphous	Grey	4.44	118	7.4 (0.5)	1.0 (0.1)	817	7.88	841	974	1063
Er	2.83	3 : 3 : 2	Amorphous	Wine	5.35	144	9.2 (0.4)	1.4 (0.1)	900	7.55	914	1063	1139
		3.45 : 3 : 2	Amorphous	Wine	5.70	151	9.2 (0.3)	1.4 (0.1)	905	7.67	913	1056	1146
Yb	2.95	3 : 3 : 2	Amorphous	Brown	5.58	143	8.9 (0.3)	1.3 (0.1)	854	7.36	881	1083	1190

where l_0 is the original length, Δl is the change in length of the specimen and ΔT is the temperature change. The inflexion point of the expansion curve was taken as the glass transition temperature ($T_{g_{Dil}}$).

2.2.3. X-ray diffraction (XRD)

Samples were prepared for powder X-ray diffraction (XRD) by crushing in a pestle and mortar and were then characterised using an X-ray powder diffractometer with Cu Kα radiation (X'Pert, Philips). Traces were compared with standards from ICDD database and data available in the literature [8, 17] in order to identify the crystalline phases present in the samples.

3. Results and discussion

3.1. Glass characterisation

Glass formation was checked by X-ray diffraction analysis. All the compositions were observed to be X-ray amorphous and different colours were observed depending on the rare-earth metal (Y, Ce, Er, Yb) cation used. Physical, mechanical and thermal properties measured on the glasses are presented in Table I. As expected, density increases with an increase in the rare-earth content, (Y and Er glasses), and with the increase of the rare-earth atomic number, Y, Ce, Er, Yb, (3 : 3 : 2 compositions).

Results obtained for the mechanical properties, Young's modulus (E), hardness (H_v) and fracture toughnes (K_{IC}) are very similar for the different compositions with the exception of the Ce glass which showed a significantly lower value. In order to analyse the effect of the rare-earth, the cationic field strengths CFS, calculated using Shannon's values [18] and valence $Z = 3$ [19] have also been included in Table I. The fact that Ce exhibits a lower CFS value 2.27 $Å^{-2}$ in comparison with 2.77, 2.83 and 2.95 for Y, Er and Yb respectively can be easily correlated with the decrease in the mechanical properties. In relation to the thermal properties, Ce glass also shows lower values for T_g and higher thermal expansion coefficient (α) for the 3 : 3 : 2 composition. Thermal expansion increases as the rare-earth ion content increases (see Y and Er compositions).

Density observed in the Y and Er glasses increases with a rise in rare-earth content. This trend can be explained by considering the relative masses of the rare-earth ions in comparison with those of the other ions in the glasses. For a given composition, the increase in density with the increase in rare-earth atomic number is primarily due to the increased atomic weights of the rare-earth cation but it may also be due to the cationic field strength [20]. The higher values for E, H_v and K_{Ic} are coincident with an increase in the CFS. The small variation in the mechanical properties observed between Y, Er and Yb can be ascribed to the similar ionic radii for these cations. Although T_g seems to have a tendency to rise with a decrease in the radius of the rare-earth ion, the linear correlation between them observed by Ramesh *et al.* [20] has not been observed in the present glasses. The increase in expansion coefficient with increasing rare-earth ion content observed is in good agreement with published data [21, 22].

The following sections review the crystallisation products derived from heat treatment experiments of the parent glasses of Table I between 1050 and 1200°C which results in formation of glass-ceramics materials that contain both crystal-phases and residual glass. A characterisation of physical properties of these materials has been performed and is discussed in relation to the crystal phase formation.

3.2. Yttrium and erbium sialon glass-ceramics characterisation

3.2.1. X-ray analysis

XRD analysis on the heat treated specimens after 10 hours heat treatment has been summarised in Table II. The Y and Er glasses crystallised with formation of I_w-phase, but the range of temperatures over which it appears as a single phase varies with composition. The 3 : 3 : 2 parent glass composition produces a single I_w-phase in the range of temperature between 1050 and 1150°C. I_w-phase is also formed in the 3.45 : 3 : 2 composition but the range of temperature over which it appears as a single phase is shifted to the range 1100–1200°C for the Y material and restricted to 1100–1150°C for the Er glass-ceramic. Weak peaks corresponding to B-phase were detected at the lower temperature of 1050°C. The non-existence of any crystalline phase other than I_w in the range of 1100–1150°C for this 3.45 : 3 : 2 composition has been confirmed by TEM studies for both Y and Er materials and reported elsewhere [23]. The Y 4 : 3 : 2 composition crystallises as a mixture of I_w-phase and B-phase between 1100 and 1150°C and the Y 4 : 3.37 : 1.5 composition produces a multiphase assemblage containing I_w-phase, B-phase and δ-$Y_2Si_2O_7$ at 1150°C. Fig. 1 shows the different parent glass compositions used, B-phase [8] and I_w-phase [9, 23] stoichiometry and the glass forming

TABLE II XRD analysis of crystallisation products obtained after 10 hours heat treatment at the appropriate temperature

Parent glass composition (M : Si : Al)	Heat treatment (°C)			
	1050	1100	1150	1200
Y 3 : 3 : 2	I_w (s)	I_w (s)	I_w (s)	I_w (s) + y-$Y_2Si_2O_7$ (m) + δ-$Y_2Si_2O_7$ (w)
Y 3.45 : 3 : 2	I_w (s) + B (w)	I_w (s)	I_w (s)	I_w (s)
Y 4 : 3 : 2	–	I_w (s) + B (m)	I_w (s) + B (w)	I_w (s) + B (w) + YAG (w) + Woll (w) + δ-$Y_2Si_2O_7$ (w)
Y 4 : 3.37 : 1.5	–	–	I_w (s) + B (m) + δ-$Y_2Si_2O_7$(m)	B (s) + δ-$Y_2Si_2O_7$(m) + y-$Y_2Si_2O_7$(m) + YAG (w) + Ap (w)
Ce 3 : 3 : 2	–	$Ce_2Si_2O_7$(s) + W(s)	$Ce_2Si_2O_7$(s) + W(s)	$Ce_2Si_2O_7$(s) + W(s)
Er 3 : 3 : 2	I_w (s)	I_w (s)	I_w (s)	I_w (s) + ErAG (s) + β-$Er_2Si_2O_7$ (s)
Er 3.45 : 3 : 2	I_w (s) + B (w)	I_w (s)	I_w (s)	I_w (s) + ErAG (s) + β-$Er_2Si_2O_7$ (s)
Yb 3 : 3 : 2	–	YbAG (s) + $Yb_2Si_2O_7$ (m) YbAM (w) + Mull (w) + $YbAlO_3$ (w) + Ap (vw)	YbAG (s) + $Yb_2Si_2O_7$ (m) + Ap (m)	YbAG (s) + $Yb_2Si_2O_7$ (m) + Ap (m)

s: strong, m: medium, w: weak, vw: very weak, –Not performed.
I_w: I_w-phase; B: B-phase, Y_2SiAlO_5N; Woll: Wollastonite, $YSiO_2N$; W: W-phase, $Ce_4Si_9Al_5O_{30}N$; Ap: N-Apatite, $Y_5Si_3O_{12}N$; YAG: $Y_3Al_5O_{12}$; LnAG: $Ln_3Al_5O_{12}$; YbAM: $Yb_4Al_2O_9$; Mull: Mullite, $Al_6Si_2O_{13}$.

region corresponding to 10 e/o N [24]. The compositions Y 4 : 3 : 2 (keeping constant the ratio Si : Al = 3 : 2) and 4 : 3.37 : 1.5 lie on the edge of the glass forming region and are closer to I_w-phase stoichiometry. However, the formation of a single I_w-phase glass-ceramic from these compositions is not possible since, multi-phase regions of I_w-phase with B-phase, or yttrium disilicate exist.

Following crystallisation at 1200°C, I_w-phase is present as a single phase only in the Y 3.45 : 3 : 2 parent glass composition. For the remainder of the compositions (see Table II) y-$Y_2Si_2O_7$, δ-$Y_2Si_2O_7$, β-$Er_2Si_2O_7$, Y or Er aluminium garnet, YAG ($Y_3Al_5O_{12}$), wollastonite ($YSiO_2N$) and apatite ($Y_5Si_3O_{12}N$) were detected at this temperature. These observations are consistent with those of Hampshire *et al*. [25] and Liddell and Thompson [3] who showed that decomposition of B and I_w-phase occurs around 1200°C to form YAG, apatite and Y disilicates.

3.2.2. Differential thermal analysis combined with X-ray difractometry on Y 3.45 : 3 : 2 parent glass composition

The crystallisation of Y 3.45 : 3 : 2 parent glass composition has been examined by a combination of differential thermal analysis and X-ray diffractometry. Fig. 2 shows the DTA profiles and the characteristic temperatures together with the normalised XRD traces showing the B-phase (002) peak and the I_w-phase (020) peak obtained after heat treatment up to 1100, 1140, 1150, 1200 and 1300°C. A heating rate of 20°C min^{-1} was chosen for these experiments in order to be consistent with that used for the 10 hours heat treatments presented in Table II. Note that characteristic temperatures for this glass, presented in Table I, correspond to experiments carried out at 5°C min^{-1}. The shift of the thermal events to higher temperatures observed in the figure is expected since an increased heating rate is used.

The DTA trace shows three thermal events. One main peak is seen at the lower temperature of 1075°C and two other less intense peaks at higher temperatures, one weak at 1119°C and another slightly more intense at 1164°C.

A characteristic B-phase diffraction pattern was obtained after heat treatment at 1100°C. The base line of the trace showed that a significant quantity of glass is still present in the sample. Heat treatment up to 1140°C shows the same B-phase diffraction pattern but with an incipient appearance of peaks corresponding to I_w-phase and the intensity of this phase increases further even at 1150°C. At 1200°C, only weak peaks corresponding to B-phase are still present and substantial transformation to I_w-phase has occurred. Since no peaks corresponding to B-phase could be detected, the transformation of B-phase into I_w-phase seems to be complete after heat treatment at 1300°C.

Fig. 3 shows normalised XRD traces of the material after heat treatment at 1100°C with holding times of 0, 0.5 and 1 hour respectively. The traces show the transformation of B-phase into I_w even after 0.5 hours heat treatment. After 1 hour only very weak intensity peaks corresponding to B-phase can be detected in the pattern. Analysis performed after 10 hours heat treatment has confirmed its complete transformation into I_w at 1100°C (Table II). The formation of I_w-phase by transformation from the previously nucleated B-phase was first suggested by Parmentier *et al*. [11]. These authors observed by SEM that I_w-phase crystallised alongside B-phase crystals suggesting that I_w grows on existing B-phase crystals. This hypothesis is corroborated by the results presented here which show the formation of B-phase as a metastable phase at lower temperature, 1100°C, and the further transformation into I_w upon increasing temperature or heat treatment time. The presence of B-phase prior to the formation of I_w-phase has also been confirmed for the Y 3 : 3 : 2 composition after a DTA heat treatment up to 1100°C.

3.2.3. Mechanical properties

Table III summarises mechanical properties measured on the M-SiAlON glass-ceramics. Standard deviations for hardness and fracture toughness are shown in brackets. Data shows small variations in density with

TABLE III Mechanical properties for M-SiAlON glass-ceramics materials (standard deviations are shown in brackets)

Parent glass composition (M : Si : Al)	Heat treatment (°C)	ρ (g cm^{-3})	E (GPa)	H_v (GPa)	K_{IC} (MPa m$^{1/2}$)
Y 3 : 3 : 2	Glass	3.89	143	8.8 (0.3)	1.4 (0.2)
	1050	3.88	175	9.7 (0.2)	1.4 (0.3)
	1100	3.93	178	9.7 (0.6)	1.1 (0.1)
	1150	3.89	176	9.9 (0.6)	1.3 (0.1)
Y 3.45 : 3 : 2	Glass	3.95	143	8.9 (0.3)	1.4 (0.1)
	1050	4.01	185	9.5 (0.2)	1.2 (0.1)
	1100	4.03	195	9.9 (0.4)	1.2 (0.1)
	1150	4.04	186	9.9 (0.2)	1.2 (0.1)
Y 4 : 3 : 2	Glass	4.12	150	–	–
	1100	4.14	195	–	–
	1150	4.13	188	–	–
	1200	4.17	188	–	–
Y 4 : 3.37 : 1.5	Glass	4.14	151	–	–
	1150	4.13	182	–	–
	1200	4.18	176	–	–
Ce 3 : 3 : 2	Glass	4.44	118	7.4 (0.5)	1.0 (0.1)
	1100	4.33	109	7.0 (0.3)	1.1 (0.3)
	1150	4.20	92	6.8 (0.3)	0.9 (0.1)
	1200	4.33	113	7.0 (0.2)	1.4 (0.2)
Er 3 : 3 : 2	Glass	5.35	144	9.2 (0.4)	1.4 (0.1)
	1050	5.46	170	9.4 (0.2)	1.3 (0.1)
	1100	5.35	170	9.7 (0.5)	1.1 (0.1)
	1150	5.43	172	9.7 (0.5)	1.3 (0.1)
Er 3.45 : 3 : 2	Glass	5.70	151	9.2 (0.3)	1.4 (0.1)
	1050	5.72	178	9.4 (0.3)	1.1 (0.1)
	1100	5.71	186	9.9 (0.5)	1.1 (0.1)
	1150	5.73	187	9.4 (0.2)	1.3 (0.1)
Yb 3 : 3 : 2	Glass	5.58	143	8.9 (0.3)	1.3 (0.1)
	1150	5.74	–	–	–
	1200	5.63	–	–	–

– Not performed.

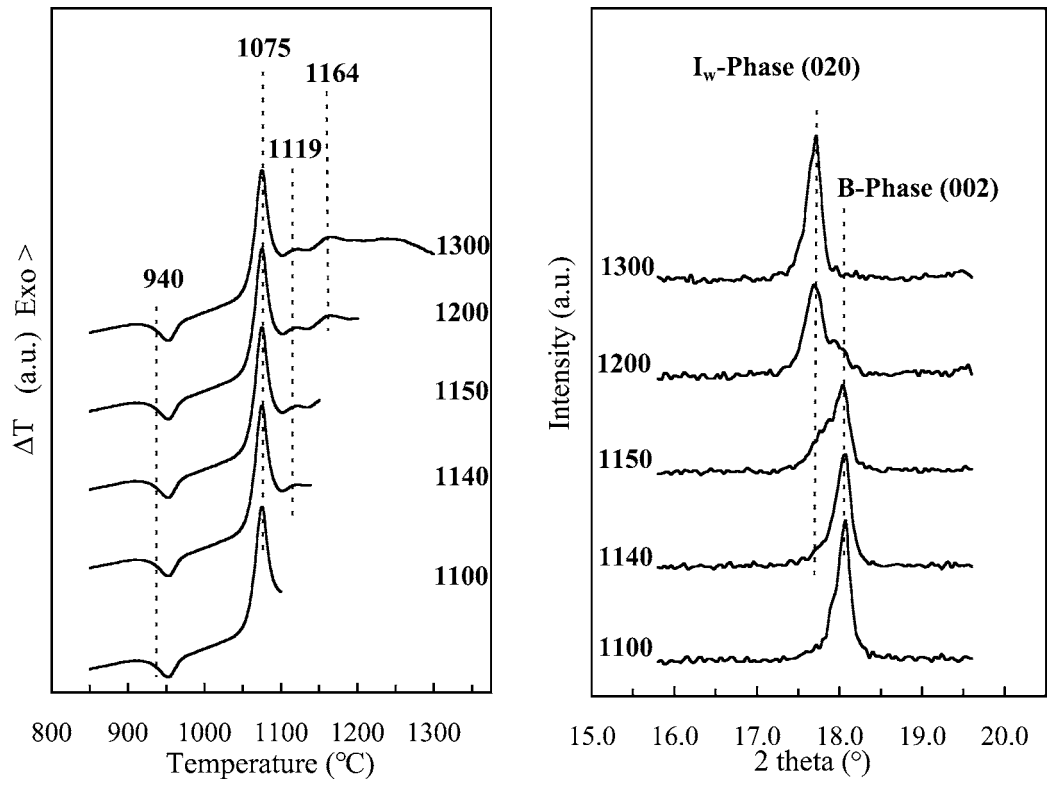

Figure 2 DTA-XRD combined analysis of Y 3.45 : 3 : 2 parent glass composition after heat treatment to 1100, 1140, 1150, 1200 and 1300°C at 20°C min^{-1}. Left: DTA traces. Right: XRD patterns.

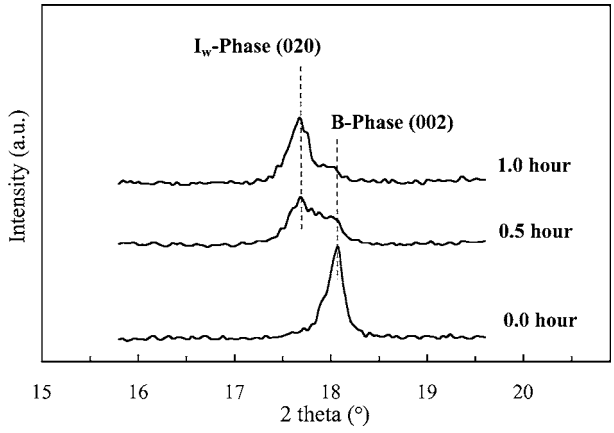

Figure 3 XRD patterns for Y 3.45 : 3 : 2 parent glass after heat treatment at 20°C min^{-1} to 1100 for 0, 0.5 and 1 hour holding times.

respect to their corresponding parent glasses. However, Young's modulus values increased significantly as a result of crystal phase formation. Rare-earth rich compositions give higher values. This increase can be correlated with the ratio of the volume of the crystal phase and the residual glass obtained by TEM [23] in which it was observed that a reduction of 5% in the residual glass occurred using the Y/Er 3.45 : 3 : 2 composition instead of the Y/Er 3 : 3 : 2 composition, in the studied range of temperature. This can be explained by the fact that the initial 3.45 : 3 : 2 glass composition is closer to the stoichiometry of the I_w crystalline phase [9, 23] as shown in Fig. 1.

The Young's modulus obtained for the Y 4 : 3 : 2 composition is similar to that measured for the Y 3.45 : 3 : 2 composition. This result is suggestive of a similar degree of crystallisation for both materials of 75% after McLaren *et al*. [23]. Using the same cation ratio parent glass composition, the increase in the heat treatment temperature from 1100 to 1150°C does not produce any significant variation in E although higher values have been obtained after heat treatment at the lower temperature. It has been shown by means of TEM observations in these materials, that an increase in the temperature from 1100 to 1150°C does not produce a change in the residual glass content but a coarsening of the microstructure [23]. Crystallites with dimensions in the range of 50–500 nm after heat treatment at 1100°C and 200–800 nm after 1150°C have been found [23]. The lower values of Young's modulus and Vickers hardness obtained for the samples heat treated at 1050°C is indicative of a lower crystal content.

Hardness values of the Y and Er I_w-glass ceramics are 5–10% higher than for parent glasses. For all the materials, the fracture toughness values obtained for the glass-ceramics are similar to those obtained for the corresponding parent glass showing that this property appears less sensitive to the crystal phase formation.

3.3. Cerium sialon glass-ceramics characterisation

Cerium disilicate ($Ce_2Si_2O_7$) and W-phase ($Ce_4Si_9Al_5O_{30}N$) [1] crystallise together in Ce 3 : 3 : 2 glasses between 1100°C and 1200°C after 10 hours heat treatment. From XRD, the intensity of the W-phase increases compared to the intensities of the $Ce_2Si_2O_7$ peaks with increasing temperature. $Ce_2Si_2O_7$ has been shown to have two polymorphic forms. The high-temperature form is monoclinic and the low temperature form is tetragonal [17, 26]. Tas *et al*. [17] observed the polymorphic transformation to take place at 1274°C in the Al_2O_3-$Ce_2Si_2O_7$ system. The heat treatment temperatures performed here (1100–1200°C) in this oxynitride system are well below the temperature reported for the formation of the high temperature form. However, XRD patterns matched the d-spacings corresponding to the monoclinic polymorph.

XRD analysis coupled with DTA experiments using a heating rate of 20°C/min are presented in Fig. 4. The glass transition temperature at 860°C and two exotherms, a first one at 998°C and a higher temperature one at 1122°C are shown in Fig. 4. Monoclinic cerium disilicate, M-$Ce_2Si_2O_7$, and cerium oxygen apatite, $Ce_{4.67}(SiO_4)_3O$ have been identified after heat treatment up to 1100°C. Heat treatment at a lower temperature, up to 1000°C, has shown the formation of $Ce_{4.67}(SiO_4)_3O$ as the only detectable crystal phase. The formation of $Ce_{4.67}(SiO_4)_3O$ as a metastable phase which disappeared upon increasing the annealing temperature has been reported in the Al_2O_3-$Ce_2Si_2O_7$ system [17] and in the early stages of densification of Si_3N_4 [27]. Upon increasing temperature or increasing the holding time M-$Ce_2Si_2O_7$ also crystallises. The DTA peak at 998°C corresponds to this.

W-phase appears after heat treatment to 1150°C which corresponds with the second cystallisation peak (1122°C). No XRD peaks corresponding to $Ce_{4.67}(SiO_4)_3O$ have been detected after treatment up to this temperature. The occurrence of W-phase at 1100°C has also been detected after a holding time of 0.5 hours.

Density, Young modulus, hardness and fracture toughness do not increase with crystallisation in cerium sialon glasses (See Table III). Stoichiometry of the crystal phases formed are far from the parent glass composition (see Fig. 1). Thermal expansion mismatch of the crystal phases and the residual glass, which has been enriched in aluminium as a result of cystallisation, can be envisaged. An increase in porosity can be deduced from the decrease in density observed with respect to the parent glass.

It has been reported that W-phase can be formed from oxygen rich rare-earth sialon glasses of approximately 1 : 2 : 1 atomic ratio [1]. The Ce 3 : 3 : 2 parent glass composition heat treated in the studied range of temperature, leads to the coexistence of W-phase and cerium disilicate. However, the same composition has produced I_w-phase in the Y and Er sialon systems. This result confirms that W-phase is more stable as the rare-earth cation size increases. W-phase has been observed previously in La, Ce and Nd systems [1].

3.4. Ytterbium sialon glass-ceramics characterisation

For the Yb 3 : 3 : 2 glass heat treated at 1100°C XRD analysis shows the formation of YAG ($Yb_3Al_5O_{12}$),

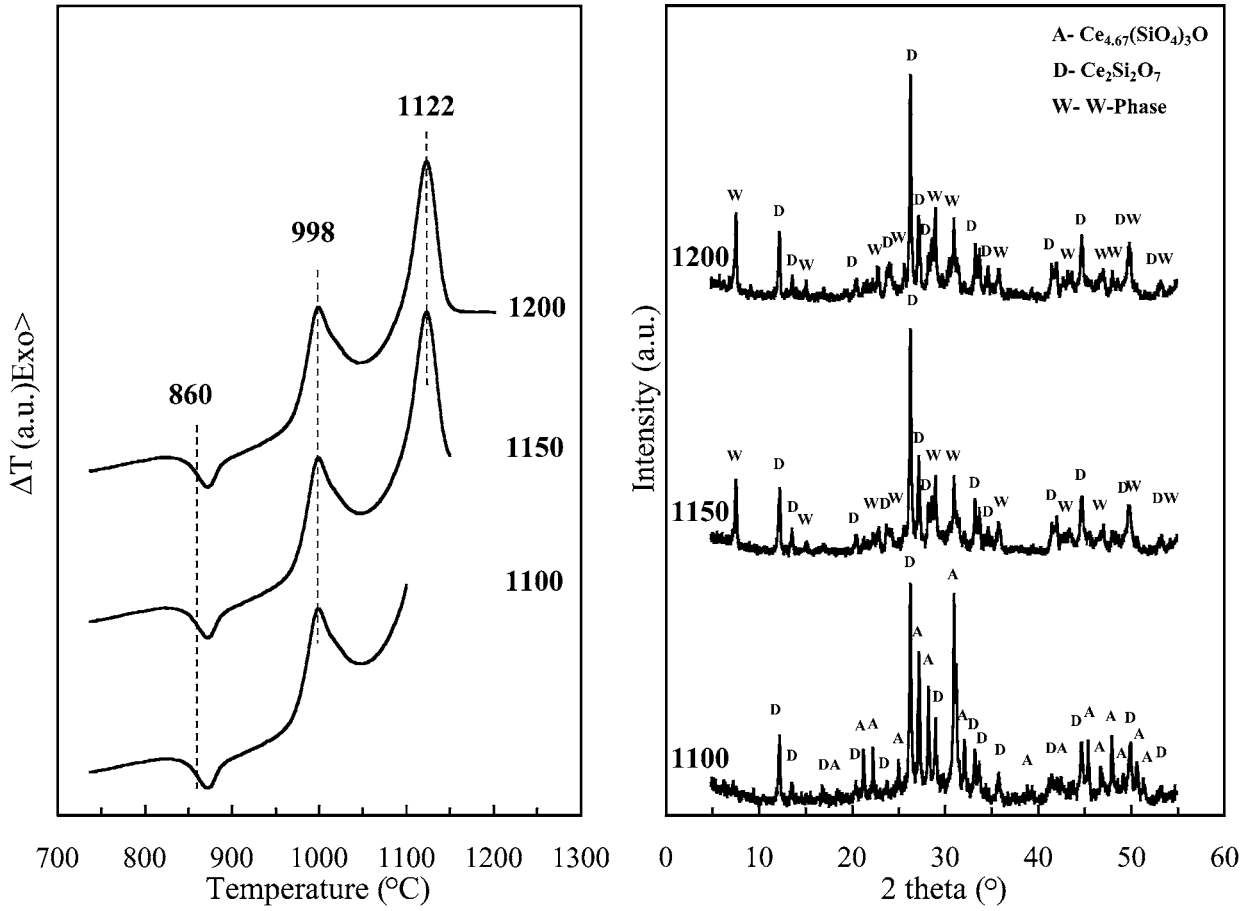

Figure 4 DTA-XRD combined analysis of Ce 3 : 2 : 2 parent glass composition after heat treatment to 1100, 1150 and 1200°C at 20°C min^{-1}. Left: DTA traces. Right: XRD patterns.

$Yb_2Si_2O_7$, YAM ($Yb_4Al_2O_9$), mullite ($Al_6Si_2O_{13}$), $YbAlO_3$ and N-Apatite ($Y_5Si_3O_{12}N$). Above this temperature, the peaks characteristic of YAM, mullite and $YbAlO_3$ disappear and, at the same time, apatite and ytterbium silicate peak intensities increase.

A strong thermal expansion mismatch as a consequence of crystallisation produced microcracked materials after heat treatment. Young's modulus could not be measured because cracks deflected the ultrasonic pulse and the echo became too weak for the measurement. The surface finish was not appropriate to perform hardness and fracture toughness by the indentation method.

I_w or B-phase have not been found in the Yb 3 : 3 : 2 material which mainly crystallises as YbAG, $Yb_2Si_2O_7$ and apatite which are more stable for this studied composition.

4. Conclusions

Glass-ceramics containing I_w-phase as the only detectable crystalline phase have been produced from $M_3Si_3Al_2O_{12.15}N_{0.90}$ and $M_{3.45}Si_3Al_2O_{12.76}N_{0.95}$ (M = Y, Er) compositions. The range of temperature over which I_w-phase forms as a pure phase has been studied. Although it is possible to obtain I_w-phase as the only existing phase from 1050 to 1200°C, this range of temperature can be reduced depending on composition.

Attempts have been made to synthesise I_w-phase from a starting glass composition closer to the I_w-phase stoichiometry. Results suggest that $M_{3.45}Si_3Al_2O_{12.76}N_{0.95}$ (M = Y, Er) is very close to an optimum composition which combines purity and maximum level of crystallinity. The formation of I_w-phase which transforms from the B-phase has also been observed.

Glass compositions $M_3Si_3Al_2O_{12.15}N_{0.90}$ (M = Ce, Yb) were prepared and heat treated to determine whether I_w-phase extends into other lanthanide sialon systems. No equivalent I_w-phase was found. Cerium silicate and W-phase were formed together in the Ce-sialon system. YAG, Ytterbium silicate, and apatite were the main phases detected in the Yb-sialon system.

Acknowledgements

The authors wish to acknowledge financial support of the European Commission under the TMR Research Networks scheme, contract number: FMRX-CT96-0038(DG 12-ORGS). The other partners and researchers in the TMR NEOCERAM network, Profs. D. P. Thompson, University of Newcastle upon Tyne, L. K. L. Falk, Chalmers University of Technology, Gothenburg, J. L. Besson, ENSCI, Limoges, P. Goursat, University of Limoges, R. K. Harris, University of Durham, F. Cambier, Belgium Ceramic Research Centre, J. D. Descamps, Ecole Polytechnique de Mons and Drs. Yvonne Menke and Ian McLaren are thanked for their encouragement and for useful discussion.

References

1. H. MANDAL, D. P. THOMPSON and T. EKSTRÖM, *Key Eng. Mater.* **72–74** (1992) 187.
2. R. RAMESH, E. NESTOR, M. J. POMEROY, S. HAMPSHIRE, K. LIDDELL and D. P. THOMPSON, *J. Non-Cryst. Solids.* **196** (1996) 320.
3. K. LIDDELL and D. P. THOMPSON, *J. Mater. Sci.* **32** (1997) 887.
4. *Idem.*, *Brit. Ceram. Trans.* **97**(4) (1998) 155.
5. H. LEMERCIER, R. RAMESH, J. L. BESSON, K. LIDDELL, D. P. THOMPSON and S. HAMPSHIRE, *Key Eng. Mater.* **132–136** (1997) 814.
6. W. T. YOUNG, L. K. L. FALK, H. LEMERCIER and S. HAMPSHIRE, *Materials Science Forum* **325–326** (2000) 289.
7. W. T. YOUNG, L. K. L. FALK, H. LEMERCIER, V. PELTIER-BARON, Y. MENKE and S. HAMPSHIRE, *J. Non-Cryst. Solids* **270** (2000) 6.
8. K. LIDDELL, H. MANDAL and D. P. THOMPSON, *J. Eur. Ceram. Soc.* **17** (1997) 781.
9. G. LENG-WARD and M. H. LEWIS, *Mater. Sci. Eng.* **71** (1985) 101.
10. *Idem.*, in "Glasses and Glass Ceramics," edited by M. H. Lewis (Chapman and Hall, London, 1989) p. 106.
11. J. PARMENTIER and D. P. THOMPSON, *Materials Science Forum* **325–326** (2000) 271.
12. S. HAMPSHIRE, R. A. L. DREW and K. H. JACK, *Phys. Chem. Glasses* **26**(5) (1985) 182.
13. J. L. BESSON, D. BILLIERS, T. ROUXEL, P. GOURSAT, R. FLYNN and S. HAMPSHIRE, *J. Am. Ceram. Soc.* **76**(8) (1993) 2103.
14. H. J. McSKIMMIN and E. S. FISHER, *J. Appl. Phys.* **31** (1960) 1627.
15. Z. LI, A. GHOSH, A. S. KOBAYASHI and R. C. BRADT, *J. Am. Ceram. Soc.* **72**(6) (1989) 904.
16. G. R. ANSTIS, P. CHANTIKUL, B. R. LAWN and D. B. MARSHALL, *ibid.* **64**(9) (1981) 533.
17. A. C. TAS and M. AKINC, *ibid.* **76**(6) (1993) 1595.
18. R. D. SHANNON and C. T. PREWITT, *Acta Cryst.* B**25** (1969) 925.
19. S. TANABE, K. HIRAO and N. SOGA, *J. Am. Ceram. Soc.* **75**(3) (1992) 503.
20. R. RAMESH, E. NESTOR, M. J. POMEROY and S. HAMPSHIRE, *J. Eur. Ceram. Soc.* **17** (1997) 1933.
21. J. T. KOHLI and J. E. SHELBY, *Phys. Chem. Glasses* **32**(2) (1991) 67.
22. E. ZHANG, K. LIDDELL and D. P. THOMPSON, *Brit. Ceram. Trans.* **95**(4) (1996) 170.
23. I. MacLAREN, L. K. L. FALK, A. DIAZ and S. HAMPSHIRE, *J. Am. Ceram. Soc.* **84**(7) (2001) 1601.
24. R. A. L. DREW, S. HAMPSHIRE and K. H. JACK in "Special Ceramics 7," British Ceramics Proceedings Vol. 31, edited by D. Taylor and P. Popper (British Ceramic Society, Stoke-on-Trent, UK, 1981) p. 119.
25. S. HAMPSHIRE, E. NESTOR, R. FLYNN, J. L. BESSON, T. ROUXEL, H. LEMERCIER, P. GOURSAT, M. SEBAI, D. P. THOMPSON and K. LIDDELL, *J. Eur. Ceram. Soc.* **14** (1994) 261.
26. A. C. TAS and M. AKINC, *J. Am. Ceram. Soc.* **77**(11) (1994) 2953.
27. T. MAH, K. S. MAZDIYASNI and R. RUH, *ibid.* **62**(1/2) (1979) 1.

Received 14 March
and accepted 16 October 2001